ABOUT SOME PRACTICAL ASPECTS OF X-RAY DIFFRACTION: FROM SINGLE CRYSTAL TO POWDERS

Carmelo Giacovazzo

Universita' di Bari, Dipartimento Geomineralogico
Via Orabona, 4 - 70125 Bari, Italy

The pages which follow are extracted from the book

FUNDAMENTALS OF CRYSTALLOGRAPHY

by

C. Giacovazzo, H. L. Monaco, D. Viterbo, F. Scordari, G. Gilli, G. Zanotti & M. Citti.
Ed. by C. Giacovazzo. By courtesy of Oxford Science Publications

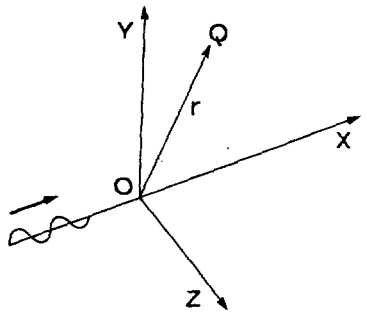

(a)

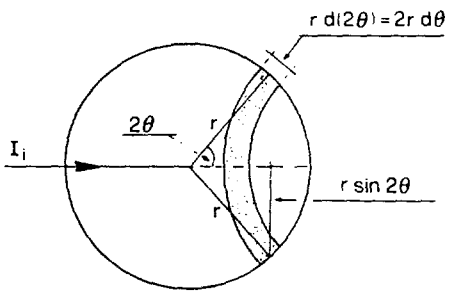

(b)

Fig. 3.1. (a) A free charged particle is in O: a plane monochromatic electromagnetic wave propagates along the x axis. (b) Surface element at scattering angle 2θ.

Thomson scattering

Let suppose that (see Fig. 3.1(a)) a free material particle with electric charge e and mass m is at the origin O of our coordinates system and that a plane monochromatic electromagnetic wave with frequency ν and electric vector $\boldsymbol{E}_i$ propagates along the x axis in positive direction. Its electric field is described by equation

$$\boldsymbol{E}_i = \boldsymbol{E}_{0i} \exp 2\pi i\nu(t - x/c)$$

where $\boldsymbol{E}_{oi}$ is the amplitude of the wave and $\boldsymbol{E}_i$ is the value of the field at position x at time t. The field exerts on the particle a periodic force $\boldsymbol{F} = e\boldsymbol{E}_i$ and therefore the particle will undergo oscillatory motion with acceleration $\boldsymbol{a} = \boldsymbol{F}/m = e\boldsymbol{E}_i/m$ and frequency ν. In accordance with classical theory of electromagnetism a charged particle in accelerated motion is a source of electromagnetic radiation: its field at $\boldsymbol{r}$ is proportional to acceleration and lies in the plane $(\boldsymbol{E}_i, \boldsymbol{r})$. Let us orient the axes y and z of our coordinates system in such a way that the observation point Q defined by vector $\boldsymbol{r}$ is in the plane (x, y). At the point Q we will measure the electric field $\boldsymbol{E}_d$ due to scattered radiation

$$\boldsymbol{E}_d = \boldsymbol{E}_{0d} \exp [2\pi i\nu(t - r/c) - i\alpha].$$

Thomson showed that (see also pp. 165–6)

$$\boldsymbol{E}_{0d} = \frac{1}{r}\boldsymbol{E}_{0i}(e^2/mc^2) \sin \varphi \qquad (3.1)$$

where φ is the angle between the direction of acceleration of electron and the direction of our observation. The term $\sin\varphi$ is a polarization term: we 'see' only the component of vibration parallel to the observer and normal to the direction of propagation. α is the phase lag with which the charge re-emits the incident radiation. The decrease of $\boldsymbol{E}_d$ with $\boldsymbol{r}$ is caused by the scattering of radiation in all directions.

In terms of intensity eqn (3.1) becomes

$$I_{eTh} = I_i \frac{e^4}{m^2 r^2 c^4} \sin^2 \varphi \tag{3.2}$$

where I_{eTh} is the density of scattered radiation and I_i is the intensity of incident radiation. This simple result excludes neutrons from the category of X-ray scatterers because they do not have electric charge, and makes negligible the contribution to scattering by protons whose factor $(e/m)^2$ is about 1837^2 times less than that of electrons. Therefore, from now on and according to tradition, the symbol e will represent the electron charge.

If the primary beam is completely polarized: (α) with $\boldsymbol{E}_i$ along the z axis, then $I_{eTh} = I_i e^4/(m^2 r^2 c^4)$; (b) with $\boldsymbol{E}_i$ along the y axis, then $\boldsymbol{E}_{eTh} = \boldsymbol{I}_i e^4 \cos^2 2\theta/(m^2 r^2 c^4)$, where 2θ is the angle between the primary beam and the direction of observation. In general, the computation can be executed by decomposing the primary beam into two beams whose electric vectors are perpendicular and parallel respectively to the plane containing the primary beam and the scattered radiation being observed. If K_1 and K_2 are parts of these two beams in percentage we obtain

$$I_{eTh} = I_i \frac{e^4}{m^2 r^2 c^4} (K_1 + K_2 \cos^2 2\theta).$$

If the primary beam is not polarized, then $K_1 = K_2 = 1/2$ and

$$I_{eTh} = I_i \frac{e^4}{m^2 r^2 c^4} \frac{1 + \cos^2 2\theta}{2} \tag{3.3}$$

where $P = (1 + \cos^2 2\theta)/2$ is called the **polarization factor** (see also p. 303). It suggests that the radiation scattered in the direction of the incident beam is maximum while it is minimum in the direction perpendicular to the primary beam.

Equation (3.3) gives the intensity scattered into a unit solid angle at angle 2θ. If we want to obtain the total scattered power P we have to integrate (3.3) from 0 to π (see Fig. 3.1(b)).

$$P = I_i \frac{e^4}{m^2 r^2 c^4} \int_0^{\pi} \frac{1 + \cos^2 2\theta}{2} 2\pi r^2 \sin 2\theta \, \mathrm{d}(2\theta)$$

$$= \frac{8\pi e^4}{3m^2 c^4} I_i$$

where $(2\pi r \sin 2\theta)\, r(\mathrm{d}(2\theta))$ is the surface element at angle 2θ. The total scattering 'cross-section' P/I_i is equal to 6.7×10^{-25} cm^2/electron, which is a very small quantity. It may be calculated that the total fraction of incident radiation scattered by one 'crystal' composed only of free electrons and having dimensions less that 1 mm is less than 2 per cent.

The scattered radiation will be partially polarized even if the incident

radiation is not. Thus, if the beam is scattered first by a crystal (monochromator) and then by the sample the polarization of the beam will be different. The scattering is coherent, according to Thomson, because there is a well defined phase relation between the incident radiation and the scattered one: for electrons $\alpha = \pi$.

Unfortunately it is very difficult to verify by experiment the Thomson formula since it is almost impossible to have a scatterer composed exclusively of free electrons. One could suppose that scatterers composed of light elements with electrons weakly bound to the nucleus is a good approximation to the ideal Thomson scatterer. But experiments with light elements have revealed a completely different effect, the Compton effect.

Compton scattering

The process can be described in terms of elastic collision between a photon and a free electron. The incident photon is deflected by a collision from its original direction and transfers a part of its energy to the electron. Consequently there is a difference in wavelength between the incident radiation and the scattered one which can be calculated by means of the relation (see also Appendix 3.B, p. 185)

$$\Delta\lambda\,(\text{Å}) = 0.024\,(1 - \cos 2\theta). \tag{3.4}$$

The following properties emerge from eqn (3.4): $\Delta\lambda$ does not depend on the wavelength of incident radiation; the maximum value of $\Delta\lambda$ ($\Delta\lambda = 0.048$) is reached for $2\theta = \pi$ (backscattering) which is small but significant for wavelengths of about 1 Å. Besides, $\Delta\lambda = 0$ for $2\theta = 0$.

Compton scattering is incoherent; it causes a variation in wavelength but does not involve a phase relation between the incident and the scattered radiation. It is impossible to calculate interference effects for Compton radiation.

Interference of scattered waves

Here we shall not be interested in wave propagation processes, but only in diffraction patterns produced by the interaction between waves and matter. These patterns are constant in time since they are produced by the system of atoms, which can be considered stationary. This fact permits us to omit the time from the wave equations.

In Fig. 3.2 two scattering centres are at O and at O′. If a plane wave excites them they become sources of secondary spherical waves which mutually interfere. Let $\boldsymbol{s}_0$ be the unit vector associated with the direction of propagation of the primary X-ray beam. The phase difference between the wave scattered by O′ in the direction defined by the unit vector $\boldsymbol{s}$ and that scattered by O in the same direction is

$$\delta = \frac{2\pi}{\lambda}(\boldsymbol{s} - \boldsymbol{s}_0)\cdot\boldsymbol{r} = 2\pi\boldsymbol{r}^*\cdot\boldsymbol{r}$$

where

$$\boldsymbol{r}^* = \lambda^{-1}(\boldsymbol{s} - \boldsymbol{s}_0). \tag{3.5}$$

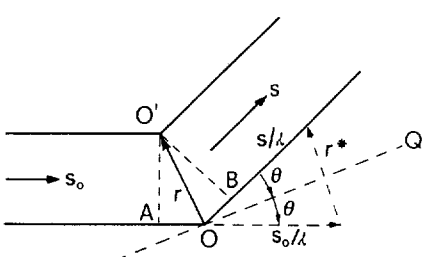

Fig. 3.2. Point scatterers are in O and O′, s_0 and s are unit vectors. Therefore AO = $-r\cdot s_0$, BO = $r\cdot s$.

If λ is much greater than r there will be no phase difference between the scattered waves and consequently no appreciable interference phenomena will occur. Since interatomic bond distances lie between 1 and 4 Å no interference effect could be observed by using visible-light waves.

The modulus of r^* can be easily derived from Fig. 3.2:

$$r^* = 2 \sin \theta/\lambda \tag{3.6}$$

where 2θ is the angle between the direction of incident X-rays and the direction of observation. If we outline two planes normal to r^* passing through O and O′ (OQ in Fig. 3.2 is the trace of the plane passing through O) we can consider interference as a consequence of specular reflection with respect to these planes.

If A_O is the amplitude of the wave scattered by the material point O (its phase is assumed to be zero) the wave scattered by O′ is described by $A_{O'} \exp(2\pi i r^* \cdot r)$. If there are N point scatterers along the path of the incident plane wave we have

$$F(r^*) = \sum_{j=1}^{N} A_j \exp(2\pi i r^* \cdot r_j) \tag{3.7a}$$

where A_j is the amplitude of the wave scattered by the jth scatterer.

The Thomson formula plays an essential role in all calculations to obtain the absolute values of scattering. In our case it is more convenient to express the intensity I scattered by a given object (for example, an atom) in terms of intensity I_{eTh} scattered by a free electron. The ratio I/I_{eTh} is f^2, where f is the **scattering factor** of the object. Vice versa, for obtaining the observed experimental intensity it is sufficient to multiply f^2 by I_{eTh}. To give an example, let us imagine a certain number of electrons concentrated at O′ which undergo Thomson scattering. In this case $f_{O'}$ expresses the number of electrons.

According to the convention stated above eqn (3.7a) becomes

$$F(r^*) = \sum_{j=1}^{N} f_j \exp(2\pi i r^* \cdot r_j). \tag{3.7b}$$

If the scattering centres constitute a continuum, the element of volume dr will contain a number of electrons equal to $\rho(r)\,\mathrm{d}r$ where $\rho(r)$ is their density. The wave scattered on the element dr is given, in amplitude and phase, by $\rho(r)\,\mathrm{d}r \exp(2\pi i r^* \cdot r)$ and the total amplitude of the scattered wave will be

$$F(r^*) = \int_V \rho(r) \exp(2\pi i r^* \cdot r)\,\mathrm{d}r = \mathrm{T}[\rho(r)] \tag{3.8}$$

where T represents the Fourier transform operator.

In crystallography the space of the r^* vectors is called **reciprocal space**. Equation (3.8) constitutes an important result: the amplitude of the scattered wave can be considered as the Fourier transform (see Appendix 3.A, p. 175) of the density of the elementary scatterers. If these are electrons, the amplitude of the scattered wave is the Fourier transform of the electron density. From the theory of Fourier transforms we also know that

$$\rho(r) = \int_{V^*} F(r^*) \exp(-2\pi i r^* \cdot r)\,\mathrm{d}r^* = \mathrm{T}^{-1}[F(r^*)]. \tag{3.9}$$

Therefore, knowledge of the amplitudes of the scattered waves (in modulus and phase) unequivocally defines $\rho(\boldsymbol{r})$.

Scattering by atomic electrons

The processes of Thomson and Compton scattering are an example of wave–particle duality and they seem to be mutually incompatible.

In fact both processes are simultaneously present and they are precisely described by modern quantum mechanics. In common practice the scatterers are atomic electrons: they can occupy different energetic states corresponding to a discontinuous set of negative energies and to a continuous band of positive energies. If, after interaction with the radiation, the electron conserves its original state the photon conserves entirely its proper energy (conditions for coherent scattering). If the electron changes its state, a portion of the energy of the incident photon is converted into potential energy of an excited atom (conditions for incoherent scattering). Quantum-mechanical calculations indicate that the processes of coherent and incoherent scattering are simultaneously present and that $I_{\text{coe}} + I_{\text{incoe}} = I_{\text{eTh}}$.

The coherent intensity I_{coe} can be calculated on the basis of the following observations. An atomic electron can be represented by its distribution function $\rho_e(\boldsymbol{r}) = |\psi(\boldsymbol{r})|^2$, where $\psi(\boldsymbol{r})$ is the wave function which satisfies the Schrödinger equation. The volume dv contains $\rho_e\, dv$ electrons and scatters an elementary wave which will interfere with the others emitted from all the elements of volume constituting the electron cloud. In accordance with p. 145 the electron scattering factor will be

$$f_e(\boldsymbol{r}^*) = \int_S \rho_e(\boldsymbol{r}) \exp(2\pi i \boldsymbol{r}^* \cdot \boldsymbol{r})\, d\boldsymbol{r} \tag{3.10}$$

where S is the region of space in which the probability of finding the electron is different from zero. If we assume that $\rho_e(\boldsymbol{r})$ has spherical symmetry (what is in fact justifiable for s electrons, less so for p, d, etc. electrons) then eqn (3.10) can be written (see eqn (3.A.33)) as:

$$f_e(r^*) = \int_0^\infty U_e(r) \frac{\sin 2\pi r r^*}{2\pi r r^*} dr \tag{3.11}$$

where $U_e(r) = 4\pi r^2 \rho_e(r)$ is the radial distribution of the electron and $r^* = 2 \sin\theta/\lambda$. For instance, there are two 1s electrons, two 2s electrons, and two 2p electrons in carbon atom. In radial approximation the 2s and 2p electrons have an equivalent distribution. For carbon the Slater formulae give

$$(\rho_e)_{1s} = \frac{c_1^3}{\pi} \exp(-2c_1 r); \qquad (\rho_e)_{2s} = \frac{c_2^5}{96\pi} r^2 \exp(-c_2 r) \tag{3.12}$$

with $c_1 = 10.77\ \text{Å}^{-1}$, $c_2 = 6.15\ \text{Å}^{-1}$. Then, eqn (3.11) gives

$$(f_e)_{1s} = \frac{c_1}{(c_1^2 + \pi^2 r^{*2})^2}, \qquad (f_e)_{2s} = \frac{c_2(c_2 - 4\pi^2 r^{*2})}{(c_2^2 + 4\pi^2 r^{*2})^4} \tag{3.13}$$

respectively.

Equation (3.12) are illustrated in Fig. 3.3(a) and eqns (3.13) in Fig. 3.3(b). In accordance with eqn (3.10) the electron scattering factor is equal to 1 when $r^* = 0$. Moreover, the scattering of 1s electrons, whose distribution is very sharp, is more efficient at higher values of r^*. If the distribution of 1s electrons could really be considered point-like their scattering factor would be constant with varying r^* (see Appendix 3.A, p. 177 for the transform of a Dirac delta function).

According to the premise of this section the intensity of the Compton radiation of an atomic electron will be

$$I_{coe} = I_{eTh}(1 - f_e^2)$$

where I_{eTh} is given by eqn (3.2) or eqn (3.3). The intensity of the Compton radiation has the same order of magnitude as the radiation scattered coherently.

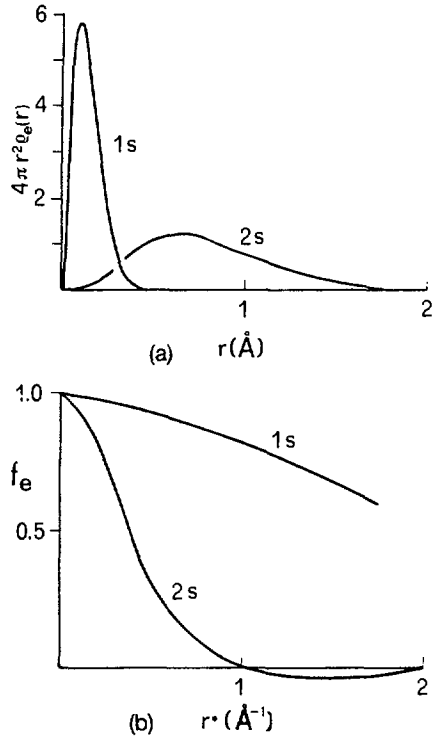

Fig. 3.3. (a) Radial distribution for 1s and 2s electrons of a C atom as defined by Slater functions. (b) ScatteRing factors for 1s and 2s electrons.

Scattering by atoms

Let $\psi_1(\boldsymbol{r}), \ldots, \psi_Z(\boldsymbol{r})$ be the wave functions of Z atomic electrons: then $\rho_{ej}\, dv = |\psi_j(\boldsymbol{r})|^2\, dv$ is the probability of finding the jth electron in the volume dv. If every function $\psi_j(\boldsymbol{r})$ can be considered independent of the others, then $\rho_a(\boldsymbol{r})\, dv = (\sum_{j=1}^{Z} \rho_{ej})\, dv$ is the probability of finding an electron in the volume dv. The Fourier transform of $\rho_a(\boldsymbol{r})$ is called the **atomic scattering factor** and will be denoted by f_a.

Generally the function $\rho_a(\boldsymbol{r})$ does not have spherical symmetry. In most crystallographic applications the deviations from it, for instance because of covalent bonds, are neglected in first approximation. If we assume that ρ_a is spherically symmetric and, without loss of generality, that the centre of the atom is at the origin, we will have

$$f_a(r^*) = \int_0^\infty U_a \frac{\sin(2\pi r r^*)}{2\pi r r^*}\, dr = \sum_{j=1}^{Z} f_{ej} \qquad (3.14)$$

where $U_a(r) = 4\pi r^2 \rho_a(r)$ is the radial distribution function for the atom. The ρ_a function is known with considerable accuracy for practically all neutral atoms and ions: for lighter atoms via Hartree–Fock methods, and for heavier atoms via the Thomas–Fermi approximation. In Fig. 3.4(a) the f_a functions for some atoms are shown. Each curve reaches its maximum value, equal to Z, at $\sin\theta/\lambda = 0$ and decreases with increasing $\sin\theta/\lambda$. According to the previous paragraph most of radiation scattered at high values of $\sin\theta/\lambda$ is due to electrons of inner shells of the electron cloud (core). Conversely scattering of valence electrons is efficient only at low $\sin\theta/\lambda$ values. f_a can thus be considered the sum of core and valence electron scattering:

$$f_a = f_{core} + f_{valence}.$$

In Fig. 3.4(b) f_{core} and $f_{valence}$ of a nitrogen atom are shown as function of $\sin\theta/\lambda$.

As a consequence of eqn (3.14) the intensity of the radiation coherently scattered from an atom can be obtained by summing the amplitudes relative

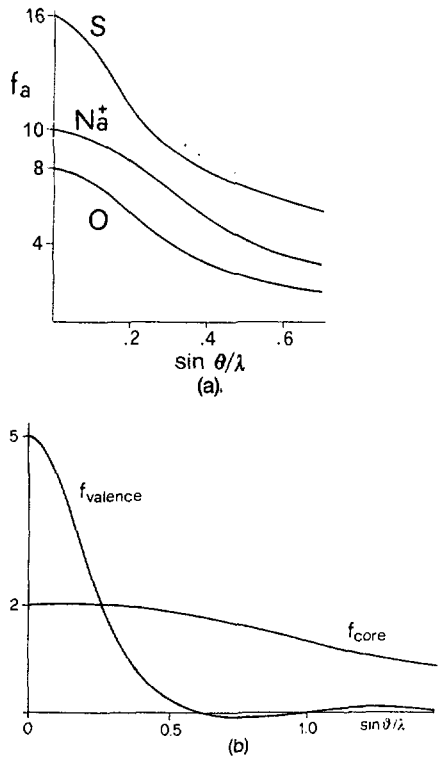

Fig. 3.4. (a) Scattering factors for S, Na^+, O. (b) core and valence scattering for nitrogen atom.

to the electrons taken individually:

$$I_{eTh} f_a^2 = I_{eTh}\left(\sum_{j=1}^{Z} f_{ej}\right)^2.$$

The Compton radiation scattered from an electron is incoherent with respect to that scattered from another electron: its intensity is obtained by summing the individual intensities relative to every single electron:

$$I_{eTh}\sum_{j=1}^{Z}[1-(f_{ej})^2].$$

Since $f_e = 1$ for $\sin\theta/\lambda = 0$ there is no Compton radiation in the direction of the primary beam. Nevertheless it is appreciable at high values of $\sin\theta/\lambda$.

When we consider the diffraction phenomenon from one crystal the intensity coherently diffracted will be proportional to the square of the vectorial sum of the amplitudes scattered from the single atoms while the intensity of the Compton radiation will be once more the sum of the single intensities. As a consequence of the very high number of atoms which contribute to diffraction, Compton scattering can generally be ignored: its presence is detectable as background radiation, easily recognizable in crystals composed of light atoms.

The temperature factor

In a crystal structure an atom is bound to others by bond forces of various types. Their arrangement corresponds to an energy minimum. If the atoms are disturbed they will tend to return to the positions of minimal energy: they will oscillate around such positions gaining thermal energy.

The oscillations will modify the electron density function of each atom and consequently their capacity to scatter. Here we will suppose that the thermal motion of an atom is independent of that of the others. This is not completely true since the chemical bonds introduce strong correlations between the thermal motions of various atoms (see pp. 117–20 and Appendix 3.B, p. 186).

The time-scale of a scattering experiment is much longer than periods of thermal vibration of atoms. Therefore the description of thermal motion of an atom requires only the knowledge of the time-averged distribution of its position with respect to that of equilibrium. If we suppose that the position of equilibrium is at the origin, that $p(\boldsymbol{r}')$ is the probability of finding the centre of one atom at $\boldsymbol{r}'$, and that $\rho_a(\boldsymbol{r}-\boldsymbol{r}')$ is the electron density at $\boldsymbol{r}$ when the centre of the atom is at $\boldsymbol{r}'$, then we can write

$$\rho_{at}(\boldsymbol{r}) = \int_{S'} \rho_a(\boldsymbol{r}-\boldsymbol{r}')p(\boldsymbol{r}')\,d\boldsymbol{r}' = \rho_a(\boldsymbol{r}') * p(\boldsymbol{r}') \qquad (3.15)$$

where $\rho_{at}(\boldsymbol{r})$ is the electron density corresponding to the thermically agitated atom. Notice that the rigid body vibration assumption has been made; i.e., the electron density is assumed to accompany the nucleus during thermal vibration.

In accordance with Appendix 3.A, p. 181), ρ_{at} is the convolution of two

functions and its Fourier transform (see eqn (3.A.38)) is

$$f_{at}(\boldsymbol{r}^*) = f_a(\boldsymbol{r}^*)q(\boldsymbol{r}^*) \tag{3.16}$$

where

$$q(\boldsymbol{r}^*) = \int_{S'} p(\boldsymbol{r}') \exp(2\pi i \boldsymbol{r}^* \cdot \boldsymbol{r}')\, d\boldsymbol{r}' \tag{3.17}$$

the Fourier transform of $p(\boldsymbol{r}')$, is known as the Debye–Waller factor.

The function $p(\boldsymbol{r}')$ depends on few parameters; it is inversely dependent on atomic mass and on chemical bond forces, and directly dependent on temperature. $p(\boldsymbol{r}')$ is in general anisotropic. If assumed isotropic, the thermal motion of the atom will have spherical symmetry and could be described by a Gaussian function in any system of reference:

$$p(\boldsymbol{r}') = p(r') \simeq (2\pi)^{-1/2} U^{-1/2} \exp[-(r'^2/2U)] \tag{3.18}$$

where r' is measured in Å and $U = \langle r'^2 \rangle$ is the square mean shift of the atom with respect to the position of equilibrium. The corresponding Fourier transform is (see eqn (3.A.25))

$$\begin{aligned} q(r^*) &= \exp(-2\pi^2 U r^{*2}) = \exp(-8\pi^2 U \sin^2\theta/\lambda^2) \\ &= \exp(-B \sin^2\theta/\lambda^2) \end{aligned} \tag{3.19}$$

where

$$B = 8\pi^2 U\ (\text{Å}^2).$$

The factor B is usually known in the literature as the **atomic temperature factor**.

The dependence of B on the absolute temperature T has been studied by Debye who obtained a formula valid for materials composed of only one chemical element. From X-ray diffraction structure analysis it is possible to conclude schematically that the order of value of $\sqrt{U}$ is in many inorganic crystals between 0.05 and 0.20 Å (B lying between 0.20 and 3.16 Å^2) but can also reach 0.5 Å ($B \simeq 20$ Å^2) for some organic crystals. The consequence of this is to make the electron density of the atom more diffuse and therefore to reduce the capacity for scattering with increasing values of $\sin\theta/\lambda$.

In general an atom will not be free to vibrate equally in all directions. If we assume that the probability $p(\boldsymbol{r}')$ has a three-dimensional Gaussian distribution the surfaces of equal probability will be ellipsoids called vibrational or thermal, centred on the mean position occupied by the atom.

Now eqn (3.19) will be substituted (see Appendix 3.B, pp. 186 and 188) by the anisotropic temperature factor (3.20) which represents a vibrational ellipsoid in reciprocal space defined by six parameters U_{11}^*, U_{22}^*, U_{33}^*, U_{12}^*, U_{13}^*, U_{23}^*:

$$\begin{aligned} q(\boldsymbol{r}^*) = \exp[-2\pi^2(&U_{11}^* x_2^* + U_{22}^* y^{*2} + U_{33}^* z^{*2} + 2U_{12}^* x^* y^* \\ &+ 2U_{13}^* x^* z^* + 2U_{23}^* y^* z^*)]. \end{aligned} \tag{3.20}$$

The six parameters U_{ij}^* (five more than the unique parameter U necessary to characterize the isotropic thermal motion) define the orientation of the thermal ellipsoid with respect to the crystallographic axes and the lengths of the three ellipsoid axes. In order to describe graphically a crystal molecule

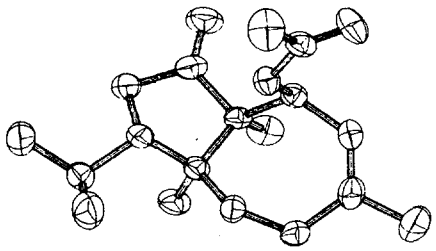

Fig. 3.5.

and its thermal motion each atom is usually represented by an ellipsoid, centred on the mean position of the atom, and surrounding the space within which the atomic displacement falls within the given ellipsoid with a probability of 0.5 (see Fig. 3.5).

Scattering by a molecule or by a unit cell

Let $\rho_j(\boldsymbol{r})$ be the electron density of the jth atom when it is thermically agitated, isolated, and localized at the origin. If the atom is at position $\boldsymbol{r}_j$ its electron density will be $\rho_j(\boldsymbol{r}-\boldsymbol{r}_j)$. If we neglect the effects of redistribution of the outer electrons because of chemical bonds, the electron density relative to an N-atom molecule or to one unit cell containing N atoms is

$$\rho_{\mathrm{M}}(\boldsymbol{r}) = \sum_{j=1}^{N} \rho_j(\boldsymbol{r}-\boldsymbol{r}_j). \tag{3.21}$$

The amplitude of the scattered wave is

$$\begin{aligned} F_{\mathrm{M}}(\boldsymbol{r}^*) &= \int_S \sum_{j=1}^{N} \rho_j(\boldsymbol{r}-\boldsymbol{r}_j) \exp(2\pi i \boldsymbol{r}^* \cdot \boldsymbol{r})\, \mathrm{d}\boldsymbol{r} \\ &= \sum_{j=1}^{N} \int_S \rho_j(\boldsymbol{R}_j) \exp[2\pi i \boldsymbol{r}^* \cdot (\boldsymbol{r}_j + \boldsymbol{R}_j)]\, \mathrm{d}\boldsymbol{R}_j \\ &= \sum_{j=1}^{N} f_j(\boldsymbol{r}^*) \exp(2\pi i \boldsymbol{r}^* \cdot \boldsymbol{r}_j), \end{aligned} \tag{3.22}$$

where $f_j(\boldsymbol{r}^*)$ is the atomic scattering factor of the jth atom (thermal motion included; in the previous section indicated by f_{at}). The fact that in eqn (3.21) we have neglected the redistribution of the outer electrons leads to negligible errors for $F_{\mathrm{M}}(\boldsymbol{r}^*)$, except in case of small r^* and for light atoms, where the number of outer electrons represents a consistent fraction of Z.

$\rho_{\mathrm{M}}(\boldsymbol{r})$, as defined by (3.21), is the electron density of a **promolecule**, or, in other words, of an assembly of spherically averaged free atoms thermically agitated and superimposed on the molecular geometry. Such a model is unsatisfactory if one is interested in the deformation of the electron density consequent to bond formation. In a real molecule the electron density is generated by superposition of molecular space orbitals ψ_i with occupation n_i:

$$\rho_{\mathrm{molecule}} = \sum_i n_i |\psi_i|^2.$$

Since ρ_{molecule} can be decomposed into atomic fragments, a finite set of appropriately chosen basis functions can be used to represent each jth atomic fragment (see Appendix 3.D). Then

$$\rho_{\mathrm{molecule}} = \rho_{\mathrm{promolecule}} + \Delta\rho$$

where $\Delta\rho$ models the effects of bonding and of molecular environment (in particular, pseudoatoms may become aspherical and carry a net charge).

By Fourier transform of $\Delta\rho$ the deformation scattering is obtained:

$$\Delta F = F_{\mathrm{molecule}} - F_{\mathrm{promolecule}}.$$

Since the core deformation scattering is negligible ΔF practically coincides with deformation scattering of the valence shells.

Diffraction by a crystal

One three-dimensional infinite lattice can be represented (see Appendix 3.A, p. 174) by the lattice function

$$L(\boldsymbol{r}) = \sum_{u,v,w=-\infty}^{+\infty} \delta(\boldsymbol{r} - \boldsymbol{r}_{u,v,w})$$

where δ is the Dirac delta function and $\boldsymbol{r}_{u,v,w} = u\boldsymbol{a} + v\boldsymbol{b} + w\boldsymbol{c}$ (with u, v, w being integers) is the generic lattice vector. Let us suppose that $\rho_M(\boldsymbol{r})$ describes the electron density in the unit cell of an infinite three-dimensional crystal. The electron density function for the whole crystal (see Appendix 3.A, p. 183) is the convolution of the $L(\boldsymbol{r})$ function with $\rho_M(\boldsymbol{r})$:

$$\rho_\infty(\boldsymbol{r}) = \rho_M(\boldsymbol{r}) * L(\boldsymbol{r}). \tag{3.23}$$

As a consequence of eqns (3.A.35), (3.A.30), and (3.22) the amplitude of the wave scattered by the whole crystal is

$$\begin{aligned} F_\infty(\boldsymbol{r}^*) &= \mathrm{T}[\rho_M(\boldsymbol{r})] \cdot \mathrm{T}[L(\boldsymbol{r})] \\ &= F_M(\boldsymbol{r}^*) \cdot \frac{1}{V} \sum_{h,k,l=-\infty}^{+\infty} \delta(\boldsymbol{r}^* - \boldsymbol{r}^*_{\mathbf{H}}) \\ &= \frac{1}{V} F_M(\mathbf{H}) \sum_{h,k,l=-\infty}^{+\infty} \delta(\boldsymbol{r}^* - \boldsymbol{r}^*_{\mathbf{H}}) \end{aligned} \tag{3.24}$$

where V is the volume of the unit cell and $\boldsymbol{r}^*_{\mathbf{H}} = h\boldsymbol{a}^* + k\boldsymbol{b}^* + l\boldsymbol{c}^*$ is the generic lattice vector of the reciprocal lattice (see pp. 63–5).

If the scatterer object is non-periodic (atom, molecule, etc.) the amplitude of the scattered wave $F_M(\boldsymbol{r}^*)$ can be non-zero for any value of $\boldsymbol{r}^*$. On the contrary, if the scatterer object is periodic (crystal) we observe a non-zero amplitude only when $\boldsymbol{r}^*$ coincides with a reciprocal lattice point:

$$\boldsymbol{r}^* = \boldsymbol{r}^*_{\mathbf{H}}. \tag{3.25}$$

The function $F_\infty(\boldsymbol{r}^*)$ can be represented by means of a pseudo-lattice: each of its points has the position coinciding with the corresponding point of the reciprocal lattice but has a specific 'weight' $F_M(\mathbf{H})/V$. For a given node the diffraction intensity $I_{\mathbf{H}}$ will be function of the square of its weight.

Let us multiply eqn (3.25) scalarly by $\boldsymbol{a}$, $\boldsymbol{b}$, $\boldsymbol{c}$ and introduce the definition (3.5) of $\boldsymbol{r}^*$: we obtain

$$\boldsymbol{a} \cdot (\boldsymbol{s} - \boldsymbol{s}_0) = h\lambda \qquad \boldsymbol{b} \cdot (\boldsymbol{s} - \boldsymbol{s}_0) = k\lambda \qquad \boldsymbol{c} \cdot (\boldsymbol{s} - \boldsymbol{s}_0) = l\lambda. \tag{3.26}$$

The directions $\boldsymbol{s}$ which satisfy eqns (3.26) are called diffraction directions and relations (3.26) are the **Laue conditions**.

Finiteness of the crystal may be taken into account by introducing the form function $\Phi(\boldsymbol{r})$: $\Phi(\boldsymbol{r}) = 1$ inside the crystal, $\Phi(\boldsymbol{r}) = 0$ outside the crystal. In this case we can write

$$\rho_{cr} = \rho_\infty(\boldsymbol{r})\Phi(\boldsymbol{r})$$

and, because of eqn (3.A.35), the amplitude of the diffracted wave is

$$F(\boldsymbol{r}^*) = \mathrm{T}[\rho_\infty(\boldsymbol{r})] * [\Phi(\boldsymbol{r})] = F_\infty(\boldsymbol{r}^*) * D(\boldsymbol{r}^*) \tag{3.27}$$

where

$$D(\boldsymbol{r}^*) = \int_S \Phi(\boldsymbol{r}) \exp(2\pi i \boldsymbol{r}^* \cdot \boldsymbol{r})\, \mathrm{d}\boldsymbol{r} = \int_\Omega \exp(2\pi i \boldsymbol{r}^* \cdot \boldsymbol{r})\, \mathrm{d}\boldsymbol{r}$$

and Ω is the volume of the crystal. Because of eqn (3.A.40) the relation (3.27) becomes

$$\begin{aligned} F(\boldsymbol{r}^*) &= \frac{1}{V} F_{\mathrm{M}}(\mathbf{H}) \sum_{h,k,l=-\infty}^{+\infty} \delta(\boldsymbol{r}^* - \boldsymbol{r}_{\mathbf{H}}^*) * D(\boldsymbol{r}^*) \\ &= \frac{1}{V} F_{\mathrm{M}}(\mathbf{H}) \sum_{h,k,l=-\infty}^{+\infty} D(\boldsymbol{r}^* - \boldsymbol{r}_{\mathbf{H}}^*). \end{aligned} \tag{3.28}$$

If we compare eqns (3.28) and (3.24) we notice that, going from an infinite crystal to a finite one, the point-like function corresponding to each node of the reciprocal lattice is substituted by the distribution function D which is non-zero in a domain whose form and dimensions depend on the form and dimensions of the crystal. The distribution D is identical for all nodes.

For example, let suppose that the crystal is a parallelepiped with faces A_1, A_2, A_3: then

$$D(\boldsymbol{r}^*) = \int_{-A_1/2}^{A_1/2} \int_{-A_2/2}^{A_2/2} \int_{-A_3/2}^{A_3/2} \exp[2\pi i(x^*x + y^*y + z^*z)]\, \mathrm{d}x\, \mathrm{d}y\, \mathrm{d}z.$$

If we integrate this function over separate variables, it becomes, in accordance with Appendix 3.A, p. 174

$$D(\boldsymbol{r}^*) = \frac{\sin(\pi A_1 x^*)}{\pi x^*} \frac{\sin(\pi A_2 y^*)}{\pi y^*} \frac{\sin(\pi A_3 z^*)}{\pi z^*}. \tag{3.29}$$

Each of the factors in eqn (3.29) is studied in Appendix 3.A and shown in Fig. 3.A.1 (p. 174). We deduce:

1. The maximum value of $D(\boldsymbol{r}^*)$ is equal to $A_1A_2A_3$, i.e. to the volume Ω of the crystal;
2. The width of a principal maximum in a certain direction is inversely proportional to the dimension of the crystal in that direction. Thus, because of the finiteness of the crystals each node of the reciprocal lattice is in practice a spatial domain with dimensions equal to A_i^{-1}. In Fig. 3.6 some examples of finite lattices with the corresponding reciprocal lattices are shown.

When we consider the diffraction by a crystal the function $F_{\mathrm{M}}(\mathbf{H})$ bears the name of **structure factor** of vectorial index $\mathbf{H}$ (or indexes h, k, l if we make reference to the components of $\boldsymbol{r}_{\mathbf{H}}^*$) and it is indicated as:

$$F_{\mathbf{H}} = \sum_{j=1}^{N} f_j \exp(2\pi i \boldsymbol{r}_{\mathbf{H}}^* \cdot \boldsymbol{r}_j)$$

where N is the number of atoms in the unit cell. In accordance with

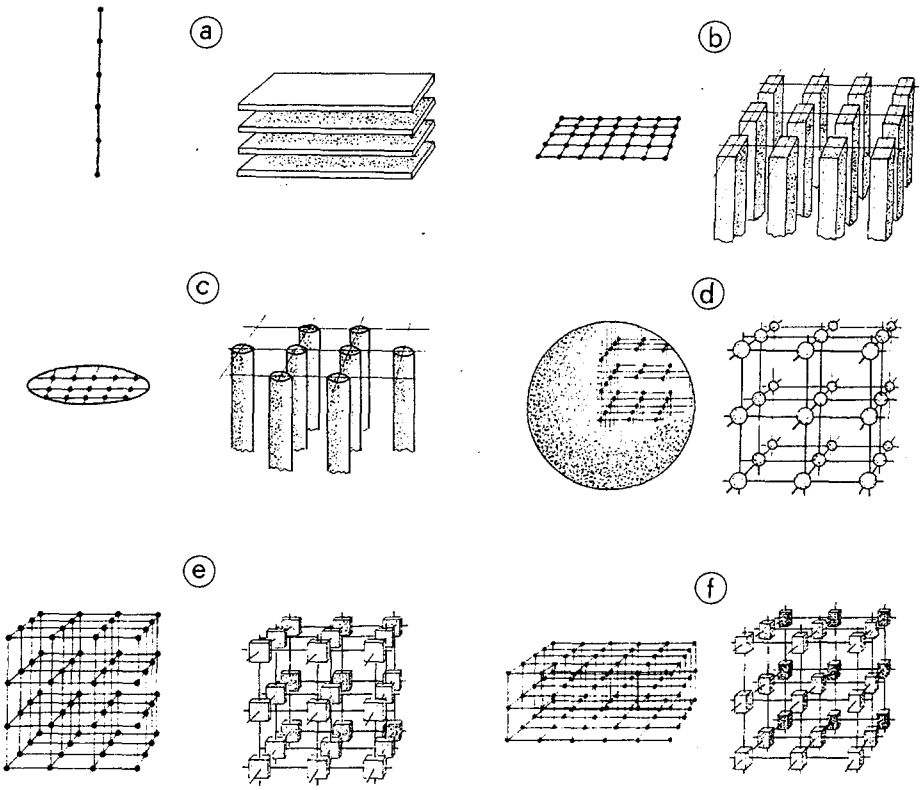

Fig. 3.6. Direct and reciprocal lattices for: (a) a one-dimensional lattice; (b) a two-dimensional lattice in the form of a rectangle; (c) a two-dimensional lattice in the form of a circle; (d) a cubic crystal in the form of a sphere; (e) a cubic crystal in the form of a cube; (f) a crystal in the form of a parallelepiped (from Kitaigorodskii, A. I. (1951). *The theory of crystal structure analysis*, Consultants Bureau, New York).

p. 64 we write

$$F_{\mathbf{H}} = \sum_{j=1}^{N} f_j \exp(2\pi \mathrm{i} \bar{\mathbf{H}} \mathbf{X}_j) = A_{\mathbf{H}} + \mathrm{i} B_{\mathbf{H}} \tag{3.30a}$$

where

$$A_{\mathbf{H}} = \sum_{j=1}^{N} f_j \cos 2\pi \bar{\mathbf{H}} \mathbf{X}_j, \qquad B_{\mathbf{H}} = \sum_{j=1}^{N} f_j \sin 2\pi \bar{\mathbf{H}} \mathbf{X}_j. \tag{3.30b}$$

According to the notation introduced in Chapter 2, we have indicated the vector as $\boldsymbol{r}_{\mathbf{H}}^*$ and the transpose matrix of its components with respect to the reciprocal coordinates system as $\bar{\mathbf{H}} = (hkl)$. In the same way $\boldsymbol{r}_j$ is the jth positional vector and the transpose matrix of its components with respect to the direct coordinates system is $\bar{\mathbf{X}}_j = [x_j\ y_j\ z_j]$. In a more explicit form (3.30a) may be written

$$F_{hkl} = \sum_{j=1}^{N} f_j \exp 2\pi \mathrm{i}(hx_j + ky_j + lz_j).$$

In different notation (see Fig. 3.7)

$$F_{\mathbf{H}} = |F_{\mathbf{H}}| \exp(\mathrm{i}\varphi_{\mathbf{H}}) \text{ where } \varphi_{\mathbf{H}} = \arctan(B_{\mathbf{H}}/A_{\mathbf{H}}). \tag{3.31}$$

$\varphi_{\mathbf{H}}$ is the **phase** of the structure factor $F_{\mathbf{H}}$.

If we want to point out in eqn (3.30a) the effect of thermal agitation of the atoms we write, in accordance with p. 149 and Appendix 3.B

$$F_{\mathbf{H}} = \sum_{j=1}^{N} f_{0j} \exp(2\pi \mathrm{i} \bar{\mathbf{H}} \mathbf{X}_j - 8\pi^2 U_j \sin^2 \theta/\lambda^2)$$

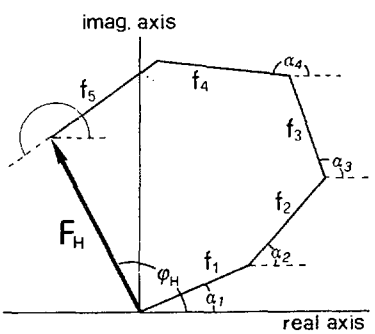

Fig. 3.7. $F_{\mathbf{H}}$ is represented in the Gauss plane for a crystal structure with $N = 5$. It is $\alpha_j = 2\pi \bar{\mathbf{H}} \mathbf{X}_j$.

or

$$F_{\mathbf{H}} = \sum_{j=1}^{N} f_{0j} \exp\left(2\pi i \bar{\mathbf{H}}\mathbf{X}_j - 2\pi^2 \bar{\mathbf{H}}\mathbf{U}_j^* \mathbf{H}\right)$$

depending on the type of the thermal motion (isotropic or anisotropic) of the atoms. f_{0j} is the scattering factor of the jth atom considered at rest. Let us note explicitly that the value of $F_{\mathbf{H}}$, in modulus and phase, depends on the atomic positions i.e. on the crystal structure.

Details of the structure factors calculation from a known structural model are given on pp. 87–8 and Appendix 2.I.

Bragg's law

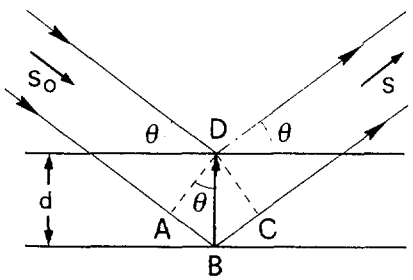

Fig. 3.8. Reflection of X-rays from two lattice planes belonging to the family $\mathbf{H} \equiv (h, k, l)$. d is the interplanar spacing.

A qualitatively simple method for obtaining the conditions for diffraction was described in 1912 by W. L. Bragg who considered the diffraction as the consequence of contemporaneous reflections of the X-ray beam by various lattice planes belonging to the same family (physically, from the atoms lying on these planes). Let θ be (see Fig. 3.8) the angle between the primary beam and the family of lattice planes with indices h, k, l (having no integer common factor larger than unity). The difference in 'path' between the waves scattered in D and B is equal to $AB + BC = 2d \sin\theta$. If it is multiple of λ then the two waves combine themselves with maximum positive interference:

$$2d_{\mathbf{H}} \sin\theta = n\lambda. \tag{3.32}$$

Since the X-rays penetrate deeply in the crystal a large number of lattice planes will reflect the primary beam: the reflected waves will interfere destructively if eqn (3.32) is not verified. Equation (3.32) is the **Bragg equation** and the angle for which it is verified is the **Bragg angle**: for $n = 1, 2, \ldots$ we obtain reflections (or diffraction effects) of first order, second order, etc., relative to the same family of lattice planes **H**.

The point of view can be further simplified by observing that the family of fictitious lattice planes with indices $h' = nh$, $k' = nk$, $l' = nl$ has interplanar spacing $d_{\mathbf{H}'} = d_{\mathbf{H}}/n$. Now eqn (3.32) can be written as

$$2(d_{\mathbf{H}}/n) \sin\theta = 2d_{\mathbf{H}'} \sin\theta = \lambda \tag{3.33}$$

where h', k', l' are no longer obliged to have only the unitary factor in common.

In practice, an effect of diffraction of nth order due to a reflection from lattice planes **H** can be interpreted as reflection of first order from the family of fictitious lattice planes $\mathbf{H}' = n\mathbf{H}$.

It is easy to see now that eqn (3.33) is equivalent to eqn (3.25). Indeed, if we consider only the moduli of eqn (3.25) we will have, because of eqns (2.14) and (3.6),

$$r^* = 2 \sin\theta/\lambda = 1/d_{\mathbf{H}}.$$

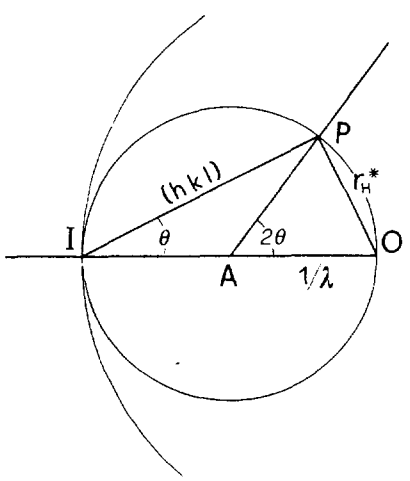

Fig. 3.9. Reflection and limiting spheres.

The reflection and the limiting spheres

Let us outline (see Fig. 3.9) a sphere of radius $1/\lambda$ in such a way that the primary beam passes along the diameter IO. Put the origin of the reciprocal

lattice at O. When the vector $r_{\mathbf{H}}^*$ is on the surface of the sphere then the corresponding direct lattice planes will lie parallely to IP and will make an angle θ with the primary beam. The relation

$$\mathrm{OP} = r_{\mathbf{H}}^* = 1/d_{\mathbf{H}} = \mathrm{IO} \sin\theta = 2 \sin\theta/\lambda$$

holds, which coincides with Bragg's equation. Therefore: the necessary and sufficient condition for the Bragg equation to be verified for the family of planes (*hkl*) is that the lattice point defined by the vector $r_{\mathbf{H}}^*$ lies on the surface of the sphere called the **reflection** or **Ewald sphere**. AP is the direction of diffracted waves (it makes an angle of 2θ with the primary beam): therefore we can suppose that the crystal is at A.

For X-rays and neutrons $\lambda \simeq (0.5\text{–}2)$ Å, which is comparable with the dimensions of the unit cell ($\simeq$10 Å): the sphere then has appreciable curvature with respect to the planes of the reciprocal lattice. If the primary beam is monochromatic and the crystal casually oriented, no point of the reciprocal lattice should be in contact with the surface of the Ewald sphere except the (000) point which represents scattering in the direction of the primary beam. It will be seen in Chapter 4 that the experimental techniques aim to bring as many nodes of the reciprocal lattice as possible into contact with the surface of the reflection sphere.

In electron diffraction $\lambda \simeq 0.05$ Å: therefore the curvature of the Ewald sphere is small with respect to the planes of the reciprocal lattice. A very high number of lattice points can simultaneously be in contact with the surface of the sphere: for instance, all the points belonging to a plane of the reciprocal lattice passing through O.

If $r_{\mathbf{H}}^* > 2/\lambda$ (then $d_{\mathbf{H}} < \lambda/2$) we will not be able to observe the reflection **H**. This condition defines the so-called **limiting sphere**, with centre O and radius $2/\lambda$: only the lattice points inside the limiting sphere will be able to diffract. Vice versa if $\lambda > 2a_{\max}$, where $a_{\max}$ is the largest period of the unit cell, then the diameter of the Ewald sphere will be smaller than $r_{\min}^*$ (the smallest period of the reciprocal lattice). Under these conditions no node could intercept the surface of the reflection sphere. That is the reason why we can never obtain diffraction of visible light (wavelength $\simeq$5000 Å) from crystals.

The wavelength determines the amount of information available from an experiment. In ideal conditions the wavelength should be short enough to leave out of the limiting sphere only the lattice points with diffraction intensities close to zero due to the decrease of atomic scattering factors.

X-ray diffraction of polycrystalline materials

An ideal polycrystalline material or powder is an ensemble of a very large number of randomly oriented crystallites. Figure 4.47 shows the effect that this random orientation has on the diffraction of a specimen assumed to contain only one reciprocal lattice node. The most remarkable difference with the single-crystal case is that we must now think of the scattering vectors not as lying on discrete nodes of reciprocal space but on the surfaces of spheres whose radii are the reciprocal lattice vectors r^*_H, the distances from the single-crystal reciprocal lattice nodes to the origin of reciprocal space. Thus, with these specimens, diffraction is observed when the scattering vectors lie at the intersection of the Ewald sphere and a series of concentric spheres centred at the reciprocal lattice origin. So, rather than having one point on the Ewald sphere, which together with the position of the sample A fixes the direction of the diffracted beam, we now have a series of circles. In strict analogy with the single-crystal case, these circles and the sample define a series of concentric cones with apex in A. The entire surface of these cones gives rise to diffraction.

A simple way to record the diffraction pattern of a polycrystalline material is by placing a film perpendicular to the incident X-ray beam. The diffraction cones will, in this case, give rise to a series of concentric rings. Alternatively, a narrow strip of film can be placed on a cylinder centred at the sample. In this case, the cones will generate concentric arcs, which are segments of the rings, on the strip. A final possibility is to reduce the strip to a line, that is to simply record the position and the intensity of the diffracted radiation on any plane that contains the incident X-ray beam. In this last case one only measures the radius of the cone and the diffracted intensity at a single position. If the sample can be considered perfectly isotropic this single measurement is sufficient to completely characterize the diffraction pattern. The parameters reported are 2θ, that is the angle made by any vector with origin in A and lying on the diffraction cone surface and the incident X-ray beam, and the relative intensity of the radiation along any direction on the cone. If the orientation of the crystallite in the specimen is not perfectly random, the pattern obtained will not be isotropic. It may even present spots corresponding to single reciprocal lattice nodes. In that case the powder sample can be appropriately rotated so that each crystallite adopts many different orientations in the course of data collection, thus generating a more homogeneous diffraction pattern. The result is equivalent to having a sample with many more possible crystallite orientations and therefore closer to isotropy. Rotation of the specimen is a standard practice in data recording of polycrystalline materials. Exceptions

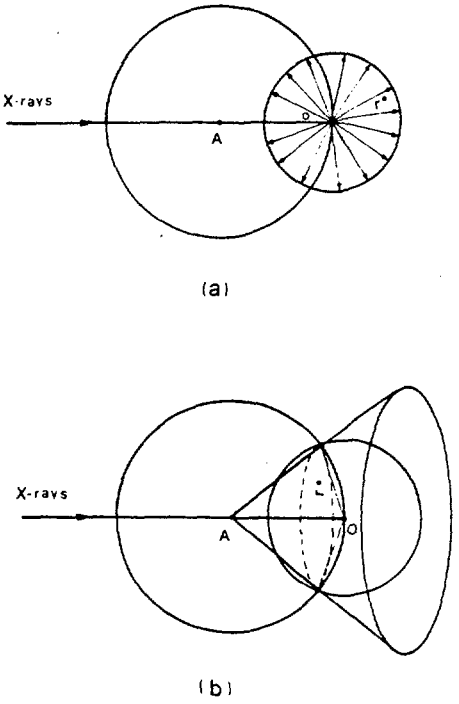

Fig. 4.47. (a) If the specimen is an aggregate of randomly oriented crystallites, the vector r^* is found in all the possible orientations with respect to the X-ray beam. These orientations define a sphere of radius r^*. (b) The intersection of the sphere of radius r^* with the Ewald sphere is a circle that together with point A defines a diffraction cone of all the possible directions in which diffraction is observed.

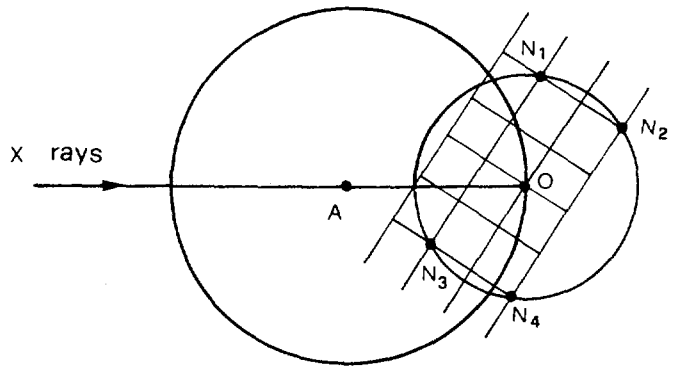

Fig. 4.48. The four reciprocal lattice nodes represented in the figure are found at the same distance from the origin of reciprocal space O and therefore they will all contribute to the intensity of the line of the cone corresponding to the distance r_i^*.

are the cases in which the preferred orientations and other properties of the crystallites need to be studied.

Another important feature which distinguishes powder diffraction is that the intensity of the diffracted radiation on the cone surfaces can arise from the contributions of more than one single-crystal reciprocal lattice node. Figure 4.48 shows in projection that this can happen both as a result of chance and crystal symmetry. A powder diffraction maximum, measured along any direction on the cone surface, is thus said to have a certain multiplicity that will be higher the higher the symmetry of the crystallites under examination.

When the diffraction experiment is performed with monochromatic radiation, that is when there only a single Ewald sphere, there is only one diffraction cone corresponding to each sphere of a given radius r_i^* in reciprocal space. In other words, the angle $2\theta_1$ corresponds unambiguously to the sphere of radius r_1^*, $2\theta_2$ to that of radius r_2^*, etc., and we have only one possibility if we want to measure the diffraction that arises from the sphere of radius r_i^*: to have some means of detecting radiation at an angle $2\theta_i$ with the incident X-ray beam. It is, however, possible to shine on the specimen X-rays with a wavelength variable within a certain range. The experiment is exactly equivalent to the Laue method used for single crystals. In this case, there will be many Ewald spheres, one for each wavelength, and each will generate a diffraction cone with a given sphere of radius r_i^*. Figure 4.49 shows the Ewald spheres corresponding to the two values limiting the wavelength interval of the radiation used. In the figure it can be seen that the diffraction due to the sphere of radius r_i^* can be measured at many different values of the angle $2\theta_i$. For different acceptable choices of $2\theta_i$ there will be diffraction produced by radiation of different wavelengths. The methods which use polychromatic incident radiation and analyse the energy or wavelength of the scattered radiation at a fixed scattering angle are called energy dispersive methods in powder diffraction. They obviously require a detector that will discriminate the energy of the arriving scattered radiation and have some advantages that make them the best choice in certain situations.[79] Just like the Laue method they are best practised with a synchrotron source which can furnish, as we have seen, radiation of adequate intensity in a rather extended energy interval. For the remainder of this chapter we will assume that we are dealing with monochromatic X-rays. The methods which use them are the most widely diffused in

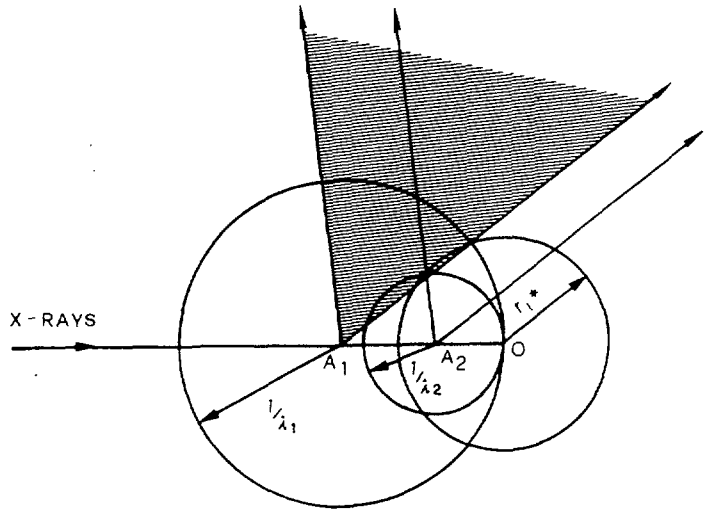

Fig. 4.49. The two Ewald spheres limiting the wavelength range of the polychromatic radiation used define with the sphere of radius r_i^* two limiting diffraction cones. All the cones in between correspond to r_i^* for different wavelengths. The shaded region in the figure shows the range of θ values that can be used to measure the diffraction in an energy dispersive experiment.

standard laboratories. From the rich literature that covers the diffraction of polycrystalline materials in depth we recommend two books.[80,81]